Self-Ratcheting Stokes Drops Driven by Oblique Vibrations

Karin John*
Laboratoire de Spectrométrie Physique UMR 5588, Université Joseph Fourier-Grenoble I, BP 87-38402 Saint-Martin-d'Hères, France
Uwe Thiele†
Department of Mathematical Sciences, Loughborough University, Loughborough, Leicestershire, LE11 3TU, United Kingdom
(Received 8 July 2009; published 8 March 2010)

We develop and analyze a minimal hydrodynamic model to understand why a drop climbs a smooth homogeneous incline that is harmonically vibrated at an angle different from the substrate normal [P. Brunet, J. Eggers, and R. D. Deegan, Phys. Rev. Lett. **99**, 144501 (2007)]. We find that the vibration component orthogonal to the substrate induces a nonlinear (anharmonic) response in the drop shape. This results in an asymmetric response of the drop to the parallel vibration and, as a consequence, in the observed net motion. In addition to establishing the basic mechanism, we identify scaling laws valid in a broad frequency range and a flow reversal at high frequencies.

DOI: 10.1103/PhysRevLett.104.107801 PACS numbers: 68.15.+e, 05.60.−k, 47.20.Ma, 68.08.Bc

The concept of transport driven by an external ratchet potential dates back to Curie [1]. He states that a locally asymmetric but globally symmetric system may induce global transport if it is kept out of equilibrium. Practical realizations include colloidal particles that may move through periodic asymmetric micropores when driven by an imposed oscillating pressure field [2]. Many different variations of ratchet mechanisms are studied today [3]. They are employed to transport or filter discrete objects [2,4] or to induce macroscopic transport of a continuous phase in systems without a macroscopic gradient [5–7]. Most modeling effort is focused on the former, but first models do exist for the latter as well [8,9].

An experiment that at first sight seems unrelated has recently shown that drops may climb an inclined homogeneous substrate if it is vibrated harmoniously in a vertical direction [10]. The experiment is quite remarkable, as previously it had only been shown that substrate vibrations can ''unlock'' drops pinned by substrate heterogeneities and therefore facilitate directed motion of drops in a global gradient [11]. A recent extension shows that drops can as well be driven by simultaneous vertical and horizontal substrate vibrations that are phase-shifted [12]. Several hypotheses have been put forward as to why the vibrations induce the drop motion. Contact angle hysteresis, nonlinear friction, anharmonicity of the vibrations, and convective momentum transport are all mentioned as possible ''minimal ingredients'' [10,12,13]. Anharmonic lateral vibrations are known to drive drop motion on horizontal substrates [14]. In general, several studies have addressed drops and free surface films on oscillating substrates since the early work by Faraday, Kelvin, and Rayleigh [15]. However, most consider fixed contact lines [16,17], purely inviscid flows [18,19], or a high frequency limit [20], and, most importantly, limit their study to vibrations either parallel or orthogonal to the substrate.

In this Letter we analyze a minimal hydrodynamic model for the situation depicted in Fig. 1 and show which of the mentioned ingredients are not necessary for the net motion of the drop. We derive a thin film evolution equation based on a Stokes flow (no convective momentum transport) for a drop on an ideally smooth homogeneous inclined substrate (no contact angle hysteresis). The obtained results show that harmonic vibrations are sufficient to drive a drop in a directed manner on a horizontal substrate [12] or as well up an incline [10]. Analyzing the underlying mechanism we find that the component of the harmonic vibration that is orthogonal to the substrate induces a nonlinear (anharmonic) response in the drop shape. As the latter determines the strongly nonlinear drop mobility, this results in an asymmetric response of the drop to the vibration component that is parallel to the substrate. The induced symmetry breaking between forward and backward motion during the different phases of the vibration results in the observed net motion of the drop. This phenomenon can be seen as a rocked self-ratcheting of the drop [3] as it is the drop itself that introduces the local time-reflection asymmetry in the response to the time-periodic driving of the sliding motion.

Next, we present our model and discuss the employed scales. The model is first analyzed in the low frequency (quasistationary) limit employing continuation techniques. Then, results for the full frequency range are obtained

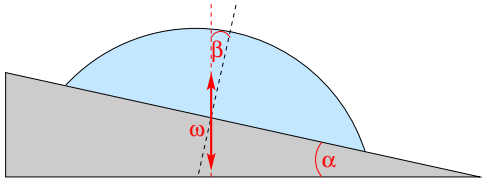

FIG. 1 (color online). Sketch of a drop on a vibrating (frequency ω, vibration angle with the substrate normal β) inclined substrate (inclination angle α).

through numerical time integration. We use a long-wave approximation [21,22] to describe the dynamics of a drop of liquid on an inclined substrate (inclination angle α) that is subject to harmonic vibrations (frequency ω, at angle β to the substrate normal, see Fig. 1). We consider a two-dimensional drop as we do not expect any conceptual difference to the three-dimensional case. The resulting evolution equation for the film thickness profile $h(x, t)$ is

$$\partial_t h = \partial_x \left[\frac{h^3}{3\eta} (\partial_x p - f) \right]. \quad (1)$$

The divergence of the flow on the right-hand side is expressed as the product of a mobility and the sum of a pressure gradient $\partial_x p$ and a lateral driving force f. η is the dynamic viscosity. The pressure

$$p = -\gamma \partial_{xx} h - \Pi(h) + \rho g h[1 + a(t)] \quad (2)$$

contains the curvature pressure $-\gamma \partial_{xx} h$, where γ denotes surface tension, and the hydrostatic pressure $\rho g h[1 + a(t)]$, where the time dependence results from the vibration component normal to the substrate. The disjoining pressure $\Pi = A[1 - (h_0/h)^3]/h^3$ models partial wettability [22,23]. Thereby, h_0 is the precursor film thickness and $A < 0$ a Hamaker constant for destabilizing van der Waals interactions [24]. The lateral force

$$f = \rho g[\alpha + \beta a(t)] \quad (3)$$

contains a constant part (force down the incline) and a time-modulated part (vibration component parallel to the substrate). The function $a(t) = a_0 \sin(\omega t)$ gives the harmonic substrate acceleration. Note that the drop experiences the opposite force; e.g., when the substrate is accelerated up and to the left, the drop is flattened and pushed to the right. Note that consistency of the long-wave approach requires small free surface slopes as well as $\alpha, |\beta| \ll 1$ [22]. However, as it is known that equations such as (1) often predict the correct behavior even for larger contact angles [21], we expect our results to hold as well for larger α and β. We introduce the scales $t_0 = 3\gamma\eta/h_0\kappa^2$, $x_0 = \sqrt{\gamma h_0/\kappa}$, and h_0 for t, x, and h, respectively, where $\kappa = |A|/h_0^3$. The resulting dimensionless problem [25] depends on the dimensionless acceleration a_0, force $G = \rho g h_0/\kappa$, period of vibration $T = 2\pi/\omega t_0$, drop volume V, and domain size L. We measure the net motion of the drop after all transients have decayed and the vibration-induced shape changes of the drop are completely periodic in time. We quantify the transport by the mean drop velocity $\langle v \rangle = \Delta x/T$, where Δx denotes the distance the drop moves within one period T.

Figure 2 illustrates the typical behavior of a drop during one vibration cycle [Fig. 2(d)]. One notices significant changes of shape [Figs. 2(a)–2(c)], and forward or backward motion [Fig. 2(e)]. The drop becomes flatter and broader [Fig. 2(b)] during the first half-cycle when it moves to the right [$t < T/2$, substrate acceleration is upward and to the left, cf. Fig. 2(e)]. In the second half-cycle the drop

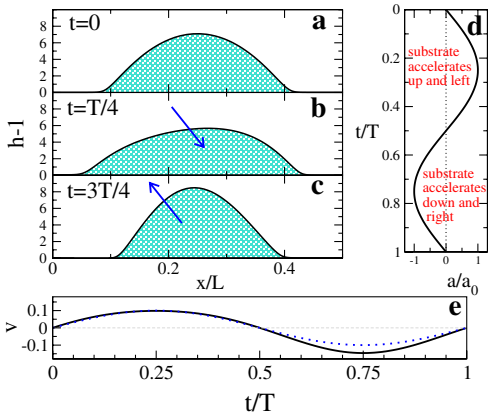

FIG. 2 (color online). Shown are (a)–(c) drop shapes at different phases of the vibration cycle. The force onto the drop due to the vibration is (a) absent at $t = 0$, (b) flattens the drop and moves it to the right (blue arrow) at $t = T/4$, and (c) makes the drop taller and moves it to the left (blue arrow) at $t = 3T/4$. After one vibration cycle typically it has moved by about 1% of its length. Panel (d) gives the substrate acceleration $a(t)/a_0$ during one cycle, whereas (e) compares the velocity during one cycle (solid line) with a harmonic variation (dotted line). Results are obtained in the low frequency limit for $V = 192$, $G = 0.001$, $\beta = 0.3$, $\alpha = 0$, $L = 128$, $a_0 = 10$.

becomes taller and less wide [Fig. 2(c)] while it moves to the left ($t > T/2$, substrate acceleration is downward and to the right). After one period the drop has moved a small net distance to the left. This can be appreciated in Fig. 2(e) where the drop velocity during the cycle (solid line) is compared with a harmonic variation (dotted line). Their difference indicates the net motion of the drop.

In the course of one period, the orthogonal component of the oblique vibration strongly modulates the hydrostatic pressure and causes a nonlinear response in the drop shape. That in turn determines the nonlinear drop mobility [$h^3/3\eta$ in Eq. (1)] and therefore induces an anharmonic response of the drop to the harmonic parallel vibration component.

The results in Fig. 2 have been obtained in the limit of low vibration frequency, i.e., when the typical time scale of the intrinsic drop dynamics t_0 is small compared to the vibration period T. In this limit the drop moves in a quasistationary manner; i.e., at each instant of the cycle its shape and velocity are those of a stationary moving drop at the corresponding constant force. The resulting moving drop solutions are parametrized by $a(t)$ and are obtained using continuation techniques [26,27]. Averaging stationary drop velocities $v(a(t))$ over one cycle gives the low frequency limit of $\langle v \rangle$.

Figure 3(a) shows the dependence of drop velocity on acceleration. The difference of the curves for positive and negative acceleration measures the anharmonic response of the drop. The mean velocity in the low frequency limit then corresponds to twice the weighted area of the shaded region in Fig. 3(a) when taken from $a = 0$ to $a = a_0$. For positive β it is directed to the left. Through a numerical analysis we find that the velocity scales as $\langle v \rangle \sim a_0^2 \beta V^{1.67}$.

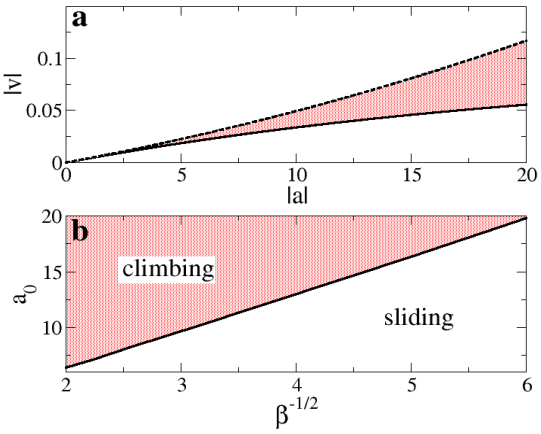

FIG. 3 (color online). Shown are for the low frequency limit: (a) the absolute value of the drop velocity depending on the absolute value of the acceleration for a horizontal substrate. The solid (dashed) line is for $a > 0$, $v > 0$ ($a < 0$, $v < 0$). (b) The phase diagram indicating the regions of sliding and climbing drops in the $\beta^{-1/2} - a_0$ plane for a substrate inclination of $\alpha = 0.1$. The remaining parameters are as in Fig. 2.

From the transport properties on a horizontal substrate it is obvious that a vibration-caused motion can overcome a further external driving and move a drop, e.g., up an incline or against a wettability gradient, as long as the product βa_0^2 is larger than a critical value. This is confirmed by the phase diagram in Fig. 3(b). There the straight line $a_0 \sim \sqrt{v_0/\beta}$ separates climbing from sliding drops, where v_0 is the drop velocity for the given substrate inclination without any vibration. Note that the case $\beta = \alpha$, i.e., a vibration vertical in the laboratory frame, is by no means special: uphill motion is generated above a finite threshold acceleration. However, in the limit $\beta \to 0$, i.e., for a vibration normal to the substrate, the threshold acceleration becomes infinite and the drop always slides down the incline.

For practical purposes, e.g., for microfluidic applications, drops need to be transported in a limited time; i.e., the behavior at sufficiently large frequencies has to be understood. We next study the full frequency range employing an adaptive time step 4th order Runge-Kutta method. Numerical instabilities are prevented by a switching upwind differencing for the driving term. The above deduced scaling $\langle v \rangle \sim a_0^2 \beta$ holds in a large frequency range. We illustrate this in Fig. 4 where dependencies of the scaled mean velocity on vibration period fall for various sets (a_0, β) onto a master curve. A second interesting feature of Fig. 4 is a reversal of the net transport at a small critical period $T_c \approx 55$. For $T < T_c$ one finds a (small) positive mean velocity even for a horizontal substrate. The reverse transport is strongest at $T_{\text{rev}} \approx T_c/2$, but always by about a factor of 10 smaller than the fastest transport to the left. Note that in agreement with the first observation T_c and T_{rev} are nearly independent of a_0 and β. They do, however, depend on drop volume (see Fig. 5), indicating that the flow reversal might be triggered when the vibration

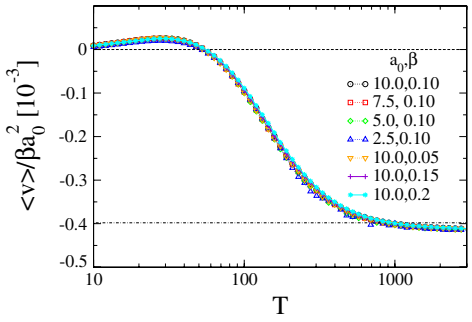

FIG. 4 (color online). Shown is for the full frequency range, the scaled mean velocity $\langle v \rangle / \beta a_0^2$ as a function of the vibration period T. The scaling allows us to "collapse" the curves for different sets (a_0, β) onto a single master curve. The lower horizontal line indicates the result in the low frequency limit. The remaining parameters are as in Fig. 2.

frequency becomes larger than an eigenfrequency of the drop; i.e., for larger imposed frequencies the response of the drop becomes delayed and phase shifted with respect to the forcing. This is corroborated by an inspection of drop profiles over the course of a cycle (not shown).

Finally, Fig. 6 presents a phase diagram that shows for fixed substrate inclination the transport direction in its dependence on the vibration period and peak acceleration. The critical acceleration $a_c(T^{-1})$ that separates sliding and climbing drops approaches a constant value at small frequencies and diverges at a finite frequency. As we do not model any effects of nonideal substrates (contact angle hysteresis, contact line pinning), our phase diagram differs in two aspects from the experimental one [10]: (i) we find a monotonic decrease of a_c with decreasing frequency whereas [10] finds evidence for a small increase at small frequencies, and (ii) here drops always slide down below a_c whereas in the experiments one finds instead a transition between static and climbing drops at large frequencies.

To conclude, we have studied a minimal hydrodynamic model for the experimentally observed drop motion that is driven by harmonic oblique substrate vibrations [10]. Our

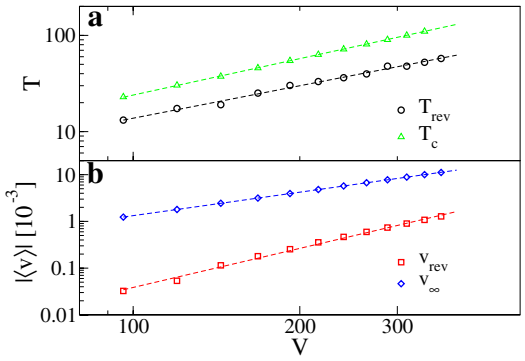

FIG. 5 (color online). Dependence of transport on drop volume: (a) shows the special vibration periods $T_{\text{rev}} \sim V^{1.12 \pm 0.03}$ and $T_c \sim V^{1.26}$; (b) gives the absolute values of the mean velocities $\langle v \rangle_{\text{rev}} \sim V^{2.78 \pm 0.06}$ at period T_{rev} and $\langle v \rangle_\infty$ at T_∞. Parameters are $G = 0.001$, $\beta = 0.1$, $\alpha = 0$, $a_0 = 10$.

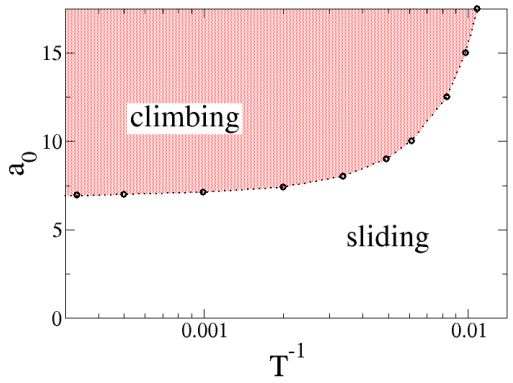

FIG. 6 (color online). Phase diagram of sliding and climbing drops in the $(a_0, 1/T)$ plane for an obliquely vibrated inclined substrate. Other than $\alpha = 0.05$, parameters are as in Fig. 2.

analysis has ruled out convective momentum transport, anharmonicity of vibrations, and contact angle hysteresis as *necessary* for the net motion. The discussed mechanism that moves drops on a horizontal substrate or even up an incline is based on a nonlinear response of the drop shape to the normal vibration component. This breaks the back and forth symmetry of the response of the drop to lateral oscillations and therefore causes a net motion. The mechanism is in line with the hypothesis put forward in [10] that a breaking of the front-back symmetry due to a nonlinear friction law is sufficient to induce transport. Here, we have identified the strongly shape-dependent nonlinear mobility in Eq. (1) as the relevant hydrodynamic ''nonlinear friction.''

In our opinion, a detailed quantitative comparison of our results obtained for two-dimensional drops in long-wave approximation (valid for small contact and vibration angles) with the experiments performed with three-dimensional drops at contact angles above $\pi/4$ [10,12] is not advisable. However, one may compare the number of vibration cycles N needed to move the drop by its own length: At a period of $T = 100$, for instance, we find a scaled mean velocity of about 10^{-4} (Fig. 4). For $a_0 = 10$ and $\beta = 0.2$ this gives $\langle v \rangle = 0.002$; i.e., for a drop such as the one in Fig. 2 one finds $N \approx 190$. An acceleration of $15g$ as in [10] would give $N \approx 90$. Typical experimental values are $N \approx 150$ ([10], at $15g$ and $f = 60$ Hz, cf. their Fig. 3) and $N \approx 50$ ([12], cf. their Figs. 1 and 2). An estimate of our time scale t_0 for water in a long-wave setting shows that $T = 100$ corresponds to frequencies of about 50 Hz. Within the limitations of long-wave theory this is a rather good agreement with the experiments.

Finally, we would like to come back to our argument that the phenomenon can be seen as a self-ratcheting of the drop as its shape changes are instrumental in producing local time-reflection asymmetries. Comparing Eq. (1) with Fokker-Planck descriptions for ratchet systems of interacting particles [3,28] one may further the analogy by noting that (i) the lateral vibration component corresponds to an imposed rocking, (ii) the orthogonal vibration component corresponds to an imposed temporal temperature modulation, (iii) the role of the spatial asymmetry in the ratchet potential is here taken by nonlinear couplings due to strongly nonlinear prefactors of the diffusion term (2nd order) and the transport term (1st order), and (iv) our surface tension term is analogous to a mean field expansion of the distribution function up to second order.

We acknowledge support by the European Union under Grant No. PITN-GA-2008-214919 (MULTIFLOW).

*kjohn@spectro.ujf-grenoble.fr
†u.thiele@lboro.ac.uk; http://www.uwethiele.de

[1] P. Curie, J. Phys. Théor. Appl. **3**, 393 (1894).
[2] S. Matthias and F. Müller, Nature (London) **424**, 53 (2003).
[3] P. Hänggi and F. Marchesoni, Rev. Mod. Phys. **81**, 387 (2009).
[4] J. Rousselet *et al.*, Nature (London) **370**, 446 (1994).
[5] A. D. Stroock *et al.*, Langmuir **19**, 4358 (2003).
[6] D. Quéré and A. Ajdari, Nature Mater. **5**, 429 (2006).
[7] A. Buguin, L. Talini, and P. Silberzan, Appl. Phys. A **75**, 207 (2002).
[8] A. Ajdari, Phys. Rev. E **61**, R45 (2000).
[9] K. John and U. Thiele, Appl. Phys. Lett. **90**, 264102 (2007).
[10] P. Brunet, J. Eggers, and R. D. Deegan, Phys. Rev. Lett. **99**, 144501 (2007).
[11] S. Daniel *et al.*, Langmuir **20**, 4085 (2004).
[12] X. Noblin, R. Kofman, and F. Celestini, Phys. Rev. Lett. **102**, 194504 (2009).
[13] E. Benilov (private communication).
[14] S. Daniel, M. K. Chaudhury, and P.-G. de Gennes, Langmuir **21**, 4240 (2005).
[15] H. Lamb, *Hydrodynamics* (Cambridge University Press, Cambridge, England, 1932).
[16] M. Strani and F. Sabetta, J. Fluid Mech. **141**, 233 (1984).
[17] F. Celestini and R. Kofman, Phys. Rev. E **73**, 041602 (2006).
[18] D. V. Lyubimov, T. P. Lyubimova, and S. V. Shklyaev, Phys. Fluids **18**, 012101 (2006).
[19] X. Noblin, A. Buguin, and F. Brochard-Wyart, Eur. Phys. J. E **14**, 395 (2004).
[20] U. Thiele, J. M. Vega, and E. Knobloch, J. Fluid Mech. **546**, 61 (2005).
[21] A. Oron, S. H. Davis, and S. G. Bankoff, Rev. Mod. Phys. **69**, 931 (1997).
[22] *Thin Films of Soft Matter*, edited by S. Kalliadasis and U. Thiele (Springer, Wien, 2007), ISBN 978-3-211-69807-5.
[23] P.-G. de Gennes, Rev. Mod. Phys. **57**, 827 (1985).
[24] L. M. Pismen, Phys. Rev. E **64**, 021603 (2001).
[25] The dimensionless equations correspond to Eqs. (1)–(3) with $3\eta = \gamma = B = 1$ and $A = -1$. Hydrostatic pressure and lateral force are $p_h = Gh[1 + a(t)]$ and $f = G[\alpha + \beta a(t)]$.
[26] E. Doedel, H. B. Keller, and J. P. Kernevez, Int. J. Bifurcation Chaos Appl. Sci. Eng. **1**, 493 (1991).
[27] U. Thiele *et al.*, Colloids Surf. A **206**, 87 (2002).
[28] S. Savel'ev, F. Marchesoni, and F. Nori, Phys. Rev. E **70**, 061107 (2004).